Diamond & Related Materials 73 (2017) 132–136

Contents lists available at ScienceDirect

Diamond & Related Materials

journal homepage: www.elsevier.com/locate/diamond

Nano-carbon pixels array for ionizing particles monitoring

S. Salvatori [a,*], P. Oliva [a,b], M. Pacilli [c], P. Allegrini [c], G. Conte [c], M. Komlenok [d], A.A. Khomich [d], A. Bolshakov [d], V. Ralchenko [d], V. Konov [d]

[a] Niccolò Cusano University, Via don Carlo Gnocchi, 3, 00166 Rome, Italy
[b] Mediterranean Institute of Fundamental Physics 'MIFP', Via Appia Nuova, 31, 00040 Marino (Rome), Italy
[c] Department of Sciences, University Roma Tre, Via della Vasca Navale, 84. 00154 Rome, Italy
[d] A.M. Prokhorov General Physics Institute, Russian Academy of Sciences, 38 Vavilova Str, 119991 Moscow, Russia

ARTICLE INFO

Article history:
Received 30 June 2016
Accepted 23 August 2016
Available online 27 August 2016

ABSTRACT

The paper deals on the response of a polycrystalline diamond sensor, 500 μm thick, to particles from a ^{90}Sr β-source. 21 × 21 nano-carbon pads, with 0.18 mm × 0.18 mm area each, were realized by ArF excimer laser irradiation on one diamond face, whereas a 7 × 7 mm^2 backside contact was fabricated and used for sensor biasing during characterization of sensor under β-source irradiation. The carbon pads embrace a number of grains, which show different degrees of surface graphitization dependent on the grain orientations. Each carbon pad exhibits a linear I(V) response up to 200 V. The average number of charge carriers collected by a single pixel, as well as the distribution of pixels involved by the impinging particle tracking, is analyzed as a function of the applied voltage recording the signals acquired by 16 pixels at a time. The pulse height distribution is not affected by reversing the bias polarity. For a single pixel, the most probable collected charge value is 1.40 ± 0.02 fC whereas the mean value gives $\langle Q\rangle_{coll} = 1.67 \pm 0.02$ fC (10,430 ± 120 electrons). The charge collection distance was measured taking into account the effect induced by high-energy electrons and found to be 285 ± 3 μm, demonstrating the absence of bulk defects induced by the laser graphitization processing. Cross-talk effects between nearest-neighbor pixels have been excluded analyzing the results obtained in a batch of more than 1000 events even if the same cannot be excluded under higher energy particles.

1. Introduction

One- and two-dimensional pixel array detectors are able to give information on both the beam position and the beam intensity profile of the impinging radiation. Even if a pixelated sensor may show a relatively high device cost, also induced by a more complex front-end electronics to be connected to each pixel, a detector made from an array of discrete sensing elements (*i.e.* photo-resistors or photo-diodes) shows several advantages if compared to other detectors [1,2]. When ionizing particles are concerned, pixel detectors are also effective to resolve the position of the impinging radiation. In such a field, poly-crystalline diamond specimens have shown their suitability [3,4]. The design of small area pixels, aimed to obtain low capacitance and a corresponding lower electronic noise amplitude, also reduces cross-talk effects between monitored signals from nearest neighbor pixels. Such features become extremely relevant in designing the processes involved in excimer laser treatment techniques used to define the active area of small tight pixels on the synthetic polycrystalline diamond [5–7].

While diamond represents a robust dielectric, under proper conditions, laser induced graphite or nano-carbon aggregates on diamond surface exhibit a strong adhesion to underneath bulk and also allow to realize electric contacts having a high conductance. However, the same optimal conditions could also produce electronic active defects in the region between adjacent pads, reducing the possibility to realize a detector having a high pixel density.

In a previous paper [4], we reported the study of a polycrystalline CVD-diamond based sensor composed of an array of 6 × 6 graphite pixels, 1 mm × 1 mm wide, fabricated by using a 248 nm KrF excimer laser irradiation. While the use of a 248 nm laser light involves the absorption towards sub-gap diamond states, phonon-assisted processes are involved when an over bandgap 193 nm laser source is concerned. In such a case the graphitization efficiency will be also dependent on the diamond grain orientation [8], which also affects material ablation and surface damage. Ablation and surface damage, as well as the threshold energy at different wavelength, have been analyzed by J. Smedley et al. [9] addressing weaker radiation laser light intensity to produce most uniform and less defected surfaces.

In this work we report the fabrication and test of a new 21 × 21 pixel array diamond detector. Each pixel, realized by means of a 193 nm ArF excimer laser, has 180 × 180 μm^2 area. Tests have been performed in

---

* Corresponding author.
E-mail address: stefano.salvatori@unicusano.it (S. Salvatori).

http://dx.doi.org/10.1016/j.diamond.2016.08.011
0925-9635/

order to demonstrate that the sensor is able to monitor β-particles emitted from a ^{90}Sr radioactive source, showing a high signal discrimination between nearest neighbor pixels and that it can be moved toward particle tracking.

2. Experimental issues

2.1. Material and laser treatment setup

The diamond sample used in this work was a commercial CVD polycrystalline diamond plate, produced by Element Six [10], having a 10 mm × 10 mm × 0.5 mm size, for which both the two diamond sides were mechanically polished by the manufacturer reducing the sample surface roughness to about 4 nm. The diamond slab was dipped in boiling $K_2Cr_2O_7$ saturated H_2SO_4 (sulphochromic) acid mixture and rinsed in aqua regia, HCl:HNO_3 (3:1), mixture in order to remove any chromium residuals [11,12]. Finally, the sample was cleaned in deionized water and isopropyl alcohol. Such a process aims to remove any conductive path from the sample surface. The diamond plate was then fixed on a motorized stage so that its nucleation side was irradiated by a pulsed UV ArF excimer laser ($\lambda = 193$ nm, $\tau = 20$ ns, CL7100 model, Optosystems Ltd.). The UV laser light beam was focused to obtain an illuminating spot having a dimension of 180 μm × 180 μm on the diamond surface, thus defining the graphitic pixel size. A squared guard ring contact (180 μm wide), surrounding the pixel array, to be connected to the same pixels potential, was also fabricated shifting the laser spot by 100 μm, allowing for a drastic decrease of the leakage current contribution from the defected diamond sample edges.

The laser light intensity on the sample surface was around 6 $J \cdot cm^{-2}$, well above the surface graphitization threshold of ≈ 2 $J \cdot cm^{-2}$ [13]. The crystallites with typical size of 10–20 μm are observed on the nucleation side of CVD-diamond (Fig. 1). The computer-controlled translation stage allowed to realize an array composed by 21 × 21 pixels, 120 μm apart along both the orthogonal directions, on the diamond nucleation side. Three consecutive laser pulses have been used to irradiate the same area to be treated.

The initial average surface roughness increased from 4 nm to 30 nm as a result of the graphitization treatment which is also accompanied by material ablation. The average thickness of the laser induced graphitized layer has been evaluated to be of about 120 nm, as measured by means of an optical profiler of a test pixel before and after chemical etching in hot sulphochromic acid mixture able to remove any graphitic specimens [11].

The Raman spectra of diamond samples taken at an excitation wavelength of 488 nm (LabRAM HR800, Horiba) after laser irradiation with the fluence above graphitization threshold usually reveal the diamond peak at 1332.5 cm^{-1} and two broad peaks around 1360 cm^{-1} (D band) and 1580 cm^{-1} (G band) assigned to disordered carbon or nano-graphite [14,15]. However, in our case intensities of these bands rather differ from one grain to another as illustrated by Fig. 2. The optical micrograph also reports a spotty pattern (Fig. 1) in which each crystallite exhibits a different blackness degree due to difference in local thickness of the graphite layer, in sp^3/sp^2 ratio and, possibly, in surface roughness.

This variation occurs due to difference in graphitization rate for different diamond crystallographic planes as known from experiments on thermal annealing of single crystal diamonds [16]. Thicker graphitic layers look brighter due to higher reflectivity of the graphite as compared to diamond. Thus, the graphite thickness (and, as a consequence, the electrical resistance of the contact) for each pixel has actually resulted as an average quantity for about the 300 grains (each with its own thickness of graphite layer determined by the grain orientation) included within a single pixel. In addition, also note that Raman spectrum of non-treated area is similar to that named "virgin" in Fig. 2 in which only the 1332 cm^{-1} diamond peak is observed.

2.2. Measurement setup

To host the matrix and the hybrid charge sensitive pre-amplifiers we used a low-noise printed circuit board (PCB). A large back graphite contact was used to attach the sample to the PCB with carbon dag. Conversely, individual pixels were wire bonded towards the amplifier inputs.

Two more slabs, 1 cm^2 large, of electronic grade polycrystalline diamond by Element Six, were coated with 8 × 8 mm^2 sputtered silver contacts (defined by means of a metal mask), 100 nm thick, and glued on independent low-noise PCB supports, with their own pre-amplifier, power supply and calibration signal input. Such two large area detectors were used to produce trigger signals in order to monitor a particle passage. The charge sensitive pre-amplifier is based on CAEN A1422H-F2, 45 mV/MeV(Si) components with an input test capacitance $C_{test} =$ 1 pF. Solid state batteries were used for low voltage ±12 V front-end amplifier power supply. A CAEN N1471A power supply was used to apply the bias voltage to the matrix using the large backside graphite

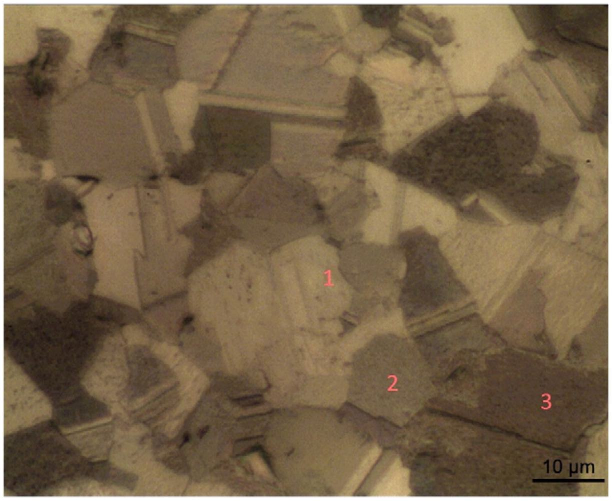

Fig. 1. A part of 180 μm × 180 μm pixel formed by laser irradiation on the nucleation side of the diamond plate (optical micrograph in reflection). Note a patchwork optical contrast picture of the surface due to the dependence of graphitization rate on grain orientation. Raman spectra for the grains #1, 2 and 3 with essentially different optical contrast are compared in Fig. 2.

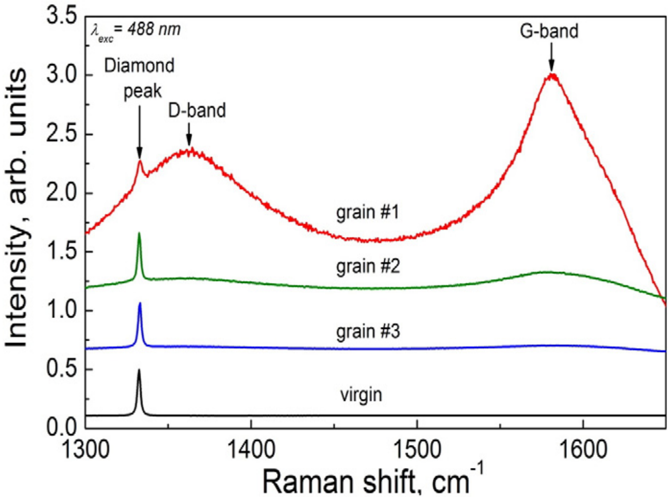

Fig. 2. Raman spectra taken in three different locations (on grains #1, 2 and 3 in Fig. 1) within the same graphitic pixel as compared with the spectrum of virgin diamond (bottom spectrum). All spectra normalized to the diamond peak intensity.